Crystal structure, hirshfeld surface analysis and inter-action energy and dft studies of 5,5-diphenyl-1,3-bis-(prop-2-yn-1-yl)imidazolidine-2,4-dione

Ismail Ghandour, Abdelouahed Bouayad, Tuncer Hokelek, Amal Haoudi, Frederic Capet, Catherine Renard, Youssef Kandri Rodi

Acta Cryst E CRYSTALLOGRAPHIC COMMUNICATIONS

ISSN 2056-9890

Crystal structure, Hirshfeld surface analysis and interaction energy and DFT studies of 5,5-diphenyl-1,3-bis(prop-2-yn-1-yl)imidazolidine-2,4-dione

Ismail Ghandour,[a] Abdelouahed Bouayad,[a] Tuncer Hökelek,[b] Amal Haoudi,[c]* Frédéric Capet,[d] Catherine Renard[d] and Youssef Kandri Rodi[c]

[a]Laboratoire de Chimie de la Matière Condensée, Université Sidi Mohamed Ben Abdallah, Faculté des Sciences et Techniques, Route d'Immouzzer, BP 2202, Fez, Morocco, [b]Department of Physics, Hacettepe University, 06800 Beytepe, Ankara, Turkey, [c]Laboratoire de Chimie Organique Appliquée, Université Sidi Mohamed Ben Abdallah, Faculté des Sciences et Techniques, Route d'Immouzzer, BP 2202, Fez, Morocco, and [d]Unité de Catalyse et de Chimie du Solide (UCCS), UMR 8181, Ecole Nationale Supérieure de Chimie de Lille, Université Lille 1, 59650 Villeneuve, d'Ascq, Cedex, France. *Correspondence e-mail: amalhaoudi2017@gmail.com

Received 15 May 2019
Accepted 30 May 2019

Edited by A. J. Lough, University of Toronto, Canada

Keywords: crystal structure; imidazolidine; oxazole; π-stacking; Hirshfeld surface.

CCDC reference: 1919743

Supporting information: this article has supporting information at journals.iucr.org/e

The title compound, $C_{21}H_{16}N_2O_2$, consists of an imidazolidine unit linked to two phenyl rings and two prop-2-yn-1-yl moieties. The imidazolidine ring is oriented at dihedral angles of 79.10 (5) and 82.61 (5)° with respect to the phenyl rings, while the dihedral angle between the two phenyl rings is 62.06 (5)°. In the crystal, intermolecular $C-H_{Prop}\cdots O_{Imdzln}$ (Prop = prop-2-yn-1-yl and Imdzln = imidazolidine) hydrogen bonds link the molecules into infinite chains along the *b*-axis direction. Two weak $C-H_{Phen}\cdots\pi$ interactions are also observed. The Hirshfeld surface analysis of the crystal structure indicates that the most important contributions for the crystal packing are from H···H (43.3%), H···C/C···H (37.8%) and H···O/O···H (18.0%) interactions. Hydrogen bonding and van der Waals interactions are the dominant interactions in the crystal packing. Computational chemistry indicates that the $C-H_{Prop}\cdots O_{Imdzln}$ hydrogen-bond energy in the crystal is −40.7 kJ mol^{-1}. Density functional theory (DFT) optimized structures at the B3LYP/6–311G(d,p) level are compared with the experimentally determined molecular structure in the solid state. The HOMO–LUMO behaviour was elucidated to determine the energy gap.

1. Chemical context

Pyrazolones are an important class of heterocyclic compounds that occur in many drugs and their derivatives have long been of interest to medicinal chemists for their wide range of biological activities (Pawar & Patil, 1994), including antibacterial, antidiabetic, immunosuppressive agents, and substances displaying hypoglycemic, antiviral and antineoplastic actions (Pathak & Bahel, 1980; Naik & Malik, 2010; Srivalli *et al.*, 2011). Their pharmaceutical applications include use as a non-steroidal anti-inflammatory agent in the treatment of arthritis and other musculoskeletal and joint disorders (Amir & Kumar, 2005), and as analgesic, antipyretic (Badawey & El-Ashmawey, 1998) and hypoglycemic agents (Das *et al.*, 2008). They also have fungicidal (Singh & Singh, 1991) and antimicrobial properties (Sahu *et al.*, 2007), and some have been tested as potential cardiovascular drugs (Higashi *et al.*, 2006). In the past few years, research has been focused on existing molecules and their modifications in order to reduce side effects and to explore other pharmacological and biological activity (Sahu *et al.*, 2007; Naik & Malik, 2010; Srivalli *et al.*, 2011). As a continuation of our research on the development of new N-substituted pyrazolone derivatives and the

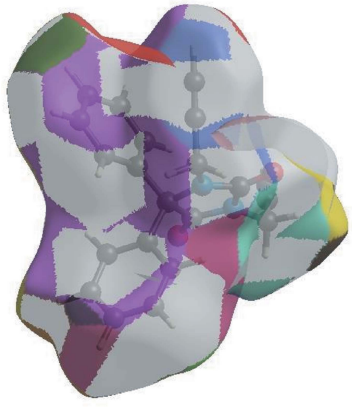

evaluation of their potential pharmacological activities, we report herein the synthesis, the molecular and crystal structures, the Hirshfeld surface analysis and intermolecular interaction energies and density functional theory (DFT) computational calculation of the title compound, (I).

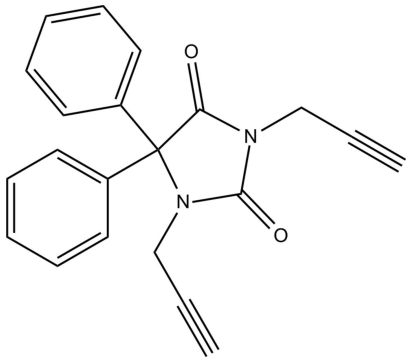

2. Structural commentary

The title molecule consists of an imidazolidine unit linked to two phenyl rings and two prop-2-yn-1-yl moieties (Fig. 1). The planar five-membered imidazolidine ring, *A* (N1/N2/C1–C3), is oriented at dihedral angles of 79.10 (5) and 82.61 (5)°, respectively, to phenyl rings *B* (C4–C9) and *C* (C10–C15), while the dihedral angle between the two phenyl rings is 62.06 (5)°. Atoms O1, O2, C16 and C19 are at distances of 0.0271 (12), −0.1040 (12), 0.1657 (19) and −0.0336 (19) Å from the mean plane of the imidazolidine ring, *A*. The orientation of the prop-2-yn-1-yl moieties with respect to the imidazolidine unit can be described by the C3—N1—C16—C17 and C3—N2—C19—C20 torsion angles of −115.3 (2) and 76.6 (2)°, respectively.

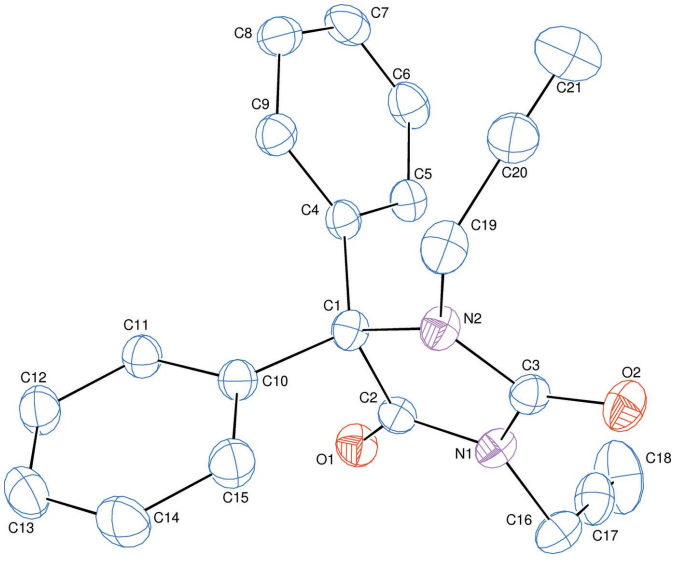

Figure 1
The molecular structure of the title compound with the atom-numbering scheme. Displacement ellipsoids are drawn at the 50% probability level.

Table 1
Hydrogen-bond geometry (Å, °).

*Cg*1 and *Cg*2 are the centroids of the C4–C9 and C10–C15 rings, respectively.

D—H···*A*	*D*—H	H···*A*	*D*···*A*	*D*—H···*A*
C16—H16*B*···O2^{vii}	0.98 (3)	2.33 (3)	3.178 (3)	144 (2)
C9—H9···*Cg*1^{vi}	0.93 (3)	2.93 (2)	3.778 (2)	152.7 (17)
C14—H14···*Cg*2^{viii}	1.00 (3)	2.87 (2)	3.762 (3)	149.6 (17)

Symmetry codes: (vi) $-x+1, y+\frac{1}{2}, -z+1$; (vii) $-x, y-\frac{1}{2}, -z$; (viii) $-x+1, y+\frac{1}{2}, -z$.

3. Supramolecular features

In the crystal, C—H$_{Prop}$···O$_{Imdzln}$ (Prop = prop-2-yn-1-yl and Imdzln = imidazolidine) hydrogen bonds (Table 1 and Fig. 2) link the molecules into infinite chains along the *b*-axis direction. Two weak C—H$_{Phen}$···π interactions (Table 1) may also contribute to the stabilization of the crystal structure.

4. Hirshfeld surface analysis

In order to visualize the intermolecular interactions in the crystal of the title compound, a Hirshfeld surface (HS) analysis (Hirshfeld, 1977; Spackman & Jayatilaka, 2009) was carried out by using *CrystalExplorer17.5* (Turner *et al.*, 2017). In the HS plotted over d_{norm} (Fig. 3), the white surface indicates contacts with distances equal to the sum of van der Waals radii, and the red and blue colours indicate distances shorter (in close contact) or longer (distinct contact) than the van der Waals radii, respectively (Venkatesan *et al.*, 2016). The bright-red spots appearing near O2 and hydrogen atom H16*B* indicate their roles as the respective donors and/or acceptors; they also appear as blue and red regions corresponding to positive and negative potentials on the HS mapped over electrostatic potential (Spackman *et al.*, 2008; Jayatilaka *et al.*, 2005) as shown in Fig. 4. The blue regions indicate the positive electrostatic potential (hydrogen-bond donors), while the red regions indicate the negative electrostatic potential

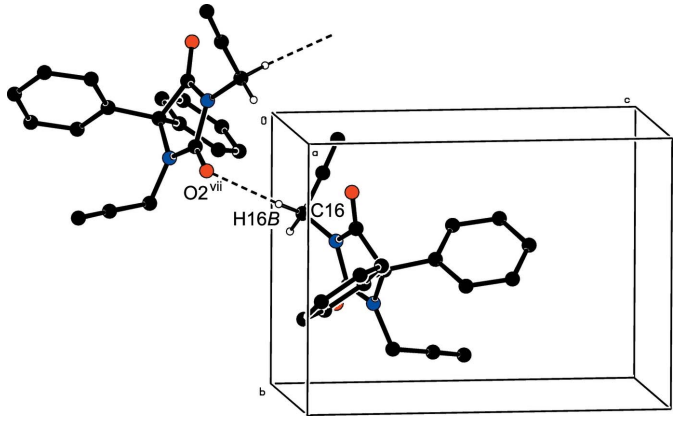

Figure 2
A partial packing diagram viewed down the *a*-axis direction. C—H$_{Prop}$···N$_{Imdzln}$ (Prop = prop-2-yn-1-yl and Imdzln = imidazolidine) hydrogen bonds (Table 1) are shown as dashed lines. Symmetry code: (vii) $-x, y-\frac{1}{2}, -z$.

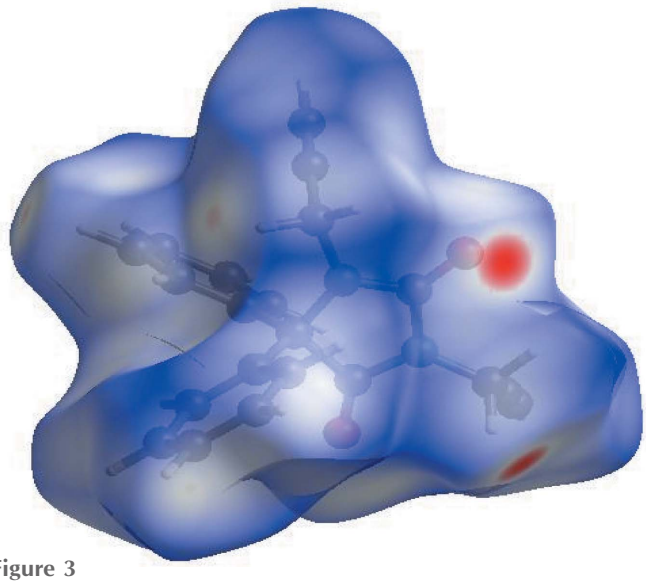

Figure 3
View of the three-dimensional Hirshfeld surface of the title compound plotted over d_{norm} in the range −0.2703 to 1.2169 a.u.

(hydrogen-bond acceptors). The shape-index of the HS is a tool to visualize the π–π stacking by the presence of adjacent red and blue triangles; if there are no adjacent red and/or blue triangles, then there are no π–π interactions. Fig. 5 clearly suggest that there are no π–π interactions in (I).

The overall two-dimensional fingerprint plot, Fig. 6*a*, and those delineated into H···H, H···C/C···H, H···O/O ··· H, C···C and H···N/N···H contacts (McKinnon *et al.*, 2007) are illustrated in Fig. 6*b–f*, together with their relative contributions to the Hirshfeld surface while details of the various contacts are given in Table 2. The most important interaction is H···H contributing 43.3% to the overall crystal packing, which is reflected in Fig. 6*b* as widely scattered points of high density due to the large hydrogen content of the molecule with the tip at $d_e + d_i$ ∼2.44 Å. In the presence of two weak C—H···π interactions, the pair of the scattered points of wings resulting from H···C/C···H contacts, with a 37.8% contribution to the HS, have a symmetrical distribution of points, Fig. 6*c*, with the thin edges at $d_e + d_i$ = 2.67 Å. The fingerprint

Table 2
Selected interatomic distances (Å).

O1···H16*B*	2.84 (2)	C4···H11	2.679 (18)
O1···H13^{i}	2.61 (2)	C6···H9^{ii}	2.97 (2)
O1···H5	2.767 (18)	C6···H18^{v}	2.90 (4)
O1···H8^{ii}	2.62 (2)	C8···H11^{vi}	2.94 (2)
O2···H18^{iii}	2.68 (5)	C8···H19*A*^{ii}	2.83 (2)
O2···H19*B*	2.65 (2)	C9···H11	2.73 (2)
O2···H16*A*	2.50 (2)	C10···H9	2.75 (2)
O2···H16*B*^{iv}	2.33 (2)	C10···H19*A*	2.96 (2)
N2···H15	2.53 (2)	C11···H14^{i}	2.94 (2)
C4···C20	3.372 (3)	C11···H9	2.79 (2)
C9···C19	3.378 (3)	C12···H14^{i}	2.91 (2)
C9···C11	3.138 (3)	C14···H7^{vi}	2.97 (2)
C9···C20	3.472 (3)	H8···H11^{vi}	2.53 (3)
C15···C19	3.450 (3)	H9···H11	2.58 (3)
C2···H5	2.476 (18)		

Symmetry codes: (i) $-x+1, y-\frac{1}{2}, -z$; (ii) $-x+1, y-\frac{1}{2}, -z+1$; (iii) $x, y+1, z$; (iv) $-x, y+\frac{1}{2}, -z$; (v) $-x, y+\frac{1}{2}, -z+1$; (vi) $-x+1, y+\frac{1}{2}, -z+1$.

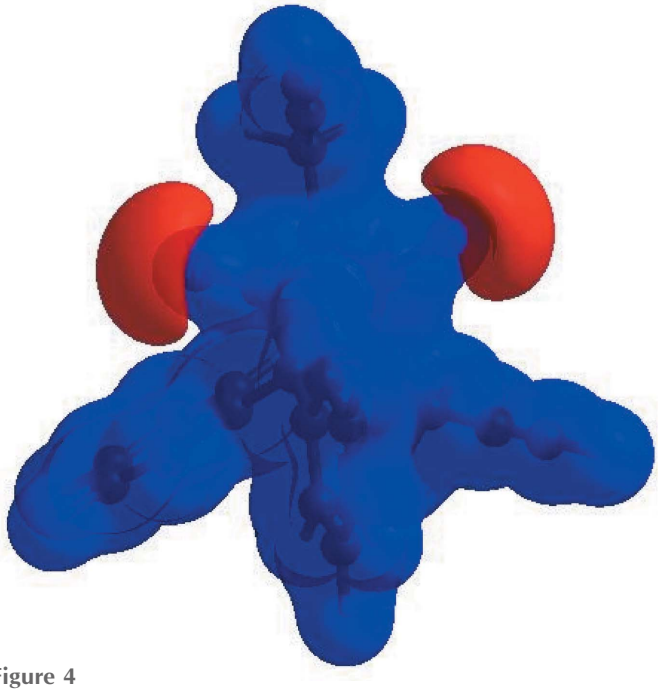

Figure 4
View of the three-dimensional Hirshfeld surface of the title compound plotted over electrostatic potential energy in the range −0.0500 to 0.0500 a.u. using the STO-3 G basis set at the Hartree–Fock level of theory. Hydrogen-bond donors and acceptors are shown as blue and red regions around the atoms corresponding to positive and negative potentials, respectively.

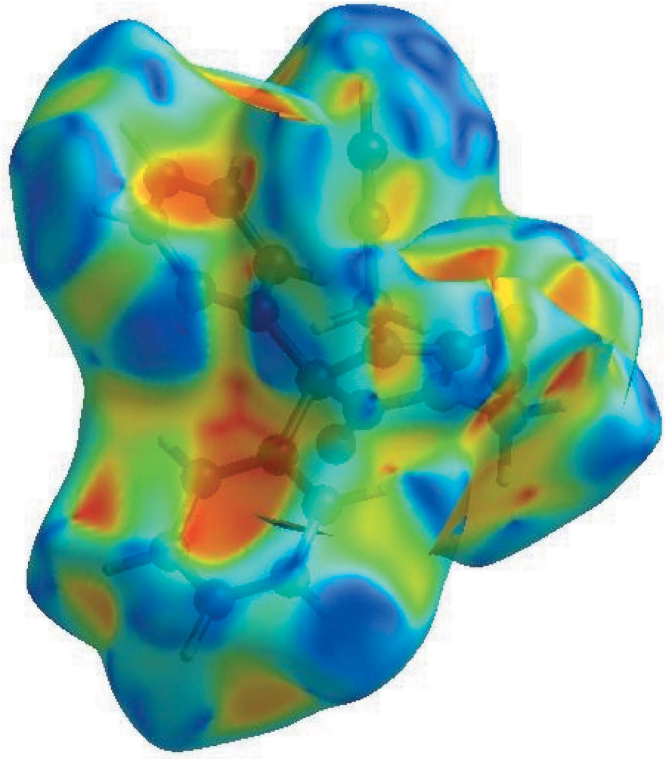

Figure 5
Hirshfeld surface of the title compound plotted over shape-index.

plot for H···O/O···H contacts (18.0% contribution), Fig. 6*d*, has a pair of spikes with the tips at $d_e + d_i = 2.24$ Å.

The Hirshfeld surface representations with the function d_{norm} plotted onto the surface are shown for the H···H, H···C/C···H and H···O/O···H interactions in Fig. 7*a–c*.

The Hirshfeld surface analysis confirms the importance of H-atom contacts in establishing the packing. The large number of H···H, H···C/C···H and H ··· O/O···H interactions suggest that van der Waals interactions and hydrogen bonding play the major roles in the crystal packing (Hathwar *et al.*, 2015).

5. Interaction energy calculations

The intermolecular interaction energies (Table 3) were calculated using the CE–B3LYP/6–311G(d,p) energy model available in *CrystalExplorer17.5* (Turner *et al.*, 2017), where a cluster of molecules is generated by applying crystallographic symmetry operations with respect to a selected central molecule within a default radius of 3.8 Å (Turner *et al.*, 2014). The total intermolecular energy (E_{tot}) is the sum of electrostatic (E_{ele}), polarization (E_{pol}), dispersion (E_{dis}) and exchange-repulsion (E_{rep}) energies (Turner *et al.*, 2015) with scale factors of 1.057, 0.740, 0.871 and 0.618, respectively (Mackenzie *et al.*, 2017). The hydrogen-bonding interaction energy (in kJ mol^{-1}) was calculated to be −15.3 (E_{ele}), −3.2 (E_{pol}), −52.2 (E_{dis}), 37.6 (E_{rep}) and −40.7 (E_{tot}) for the C—H_{Prop}···N_{Imdzln} interaction.

Table 3
Calculated energies and other parameters for (I).

Parameter	Value in (I)
Total energy E_{tot} (eV)	−30168.2025
E_{HOMO} (eV)	−6.6964
E_{LUMO} (eV)	−0.8090
Energy gap, ΔE (eV)	5.8878
Dipole moment, μ (Debye)	2.5919
Ionization potential, I (eV)	6.6964
Electron affinity, A	0.8090
Electro negativity, χ	4.0554
Hardness, η	2.9437
Electrophilicity index, ω	2.3920
Softness, σ	0.3397
Fraction of electrons transferred, ΔN	0.5516

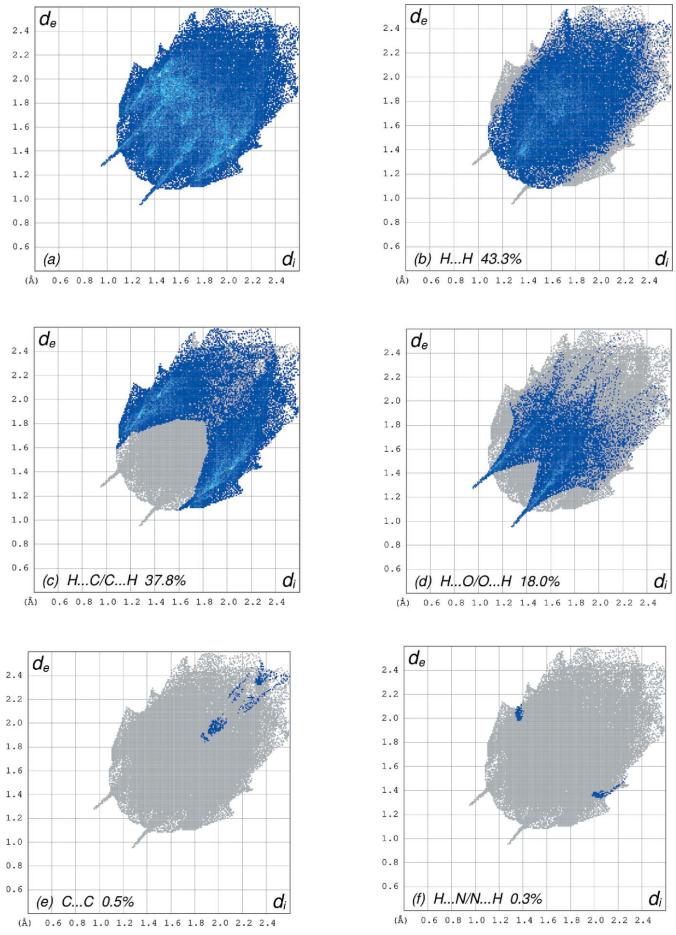

Figure 6
The full two-dimensional fingerprint plots for the title compound, showing (*a*) all interactions, and delineated into (*b*) H···H, (*c*) H···C/C···H, (*d*) H···O/O···H, (*e*) C···C and (*f*) H···N/N···H interactions. The d_i and d_e values are the closest internal and external distances (in Å) from given points on the Hirshfeld surface contacts.

6. DFT calculations

The optimized structure of the title compound in the gas phase was generated theoretically *via* density functional theory (DFT) calculations using the standard B3LYP functional and

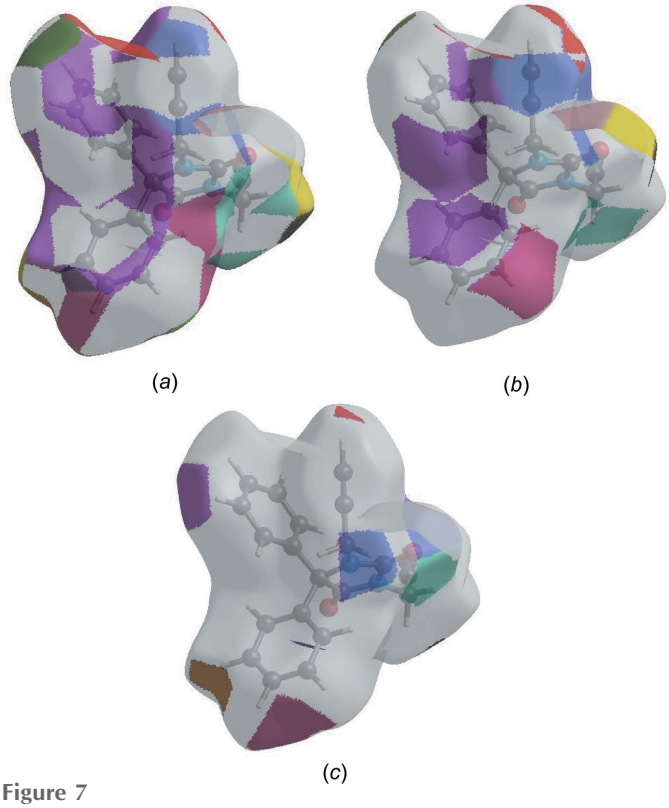

Figure 7
The Hirshfeld surface representations with the function d_{norm} plotted onto the surface for (*a*) H···H, (*b*) H···C/C···H and H···O/O ··· H interactions.

Table 4
Comparison of the selected (X-ray and DFT) geometric data (Å, °).

Bonds/angles	X-ray	B3LYP/6–311G(d,p)
O1—C2	1.203 (3)	1.237
O2—C3	1.208 (2)	1.242
N2—C3	1.346 (3)	1.379
N2—C1	1.472 (3)	1.494
N2—C19	1.454 (3)	1.470
N1—C3	1.399 (3)	1.414
N1—C2	1.360 (3)	1.384
N1—C16	1.453 (3)	1.467
C3—N2—C1	112.90 (16)	112.45
C3—N2—C19	121.81 (18)	120.14
N2—C3—N1	107.02 (17)	106.95
C3—N1—C16	122.9 (2)	122.80
C2—N1—C3	112.60 (17)	112.41
O2—C3—N2	128.0 (2)	127.88
O2—C3—N1	125.0 (2)	125.10

6–311G(d,p) basis set (Becke, 1993) as implemented in *GAUSSIAN 09* (Frisch *et al.*, 2009). The theoretical and experimental results are in good agreement (Table 4). The highest occupied molecular orbital (HOMO), acting as an electron donor, and the lowest unoccupied molecular orbital (LUMO), acting as an electron acceptor, are very important parameters for quantum chemistry. When the energy gap is small, the molecule is highly polarizable and has high chemical reactivity. The DFT calculations provide some important information on the reactivity and site selectivity of the molecular framework. E_{HOMO} and E_{LUMO} clarify the inevitable charge-exchange collaboration inside the studied material; the electronegativity (χ), hardness (η), potential (μ), electrophilicity (ω) and softness (σ) are recorded in Table 3. The significance of η and σ is to evaluate both the reactivity and stability of a compound. The electron transition from the HOMO to the LUMO energy level is shown in Fig. 8. The HOMO and LUMO are localized in the plane extending from the whole 5,5-diphenyl-1,3-di(prop-2-yn-1-yl)imidazolidine-2,4-dione ring. The energy band gap [$\Delta E = E_{LUMO} - E_{HOMO}$] of the molecule is about 5.8874 eV, and the frontier molecular orbital energies, E_{HOMO} and E_{LUMO} are −6.6964 and −0.8090 eV, respectively.

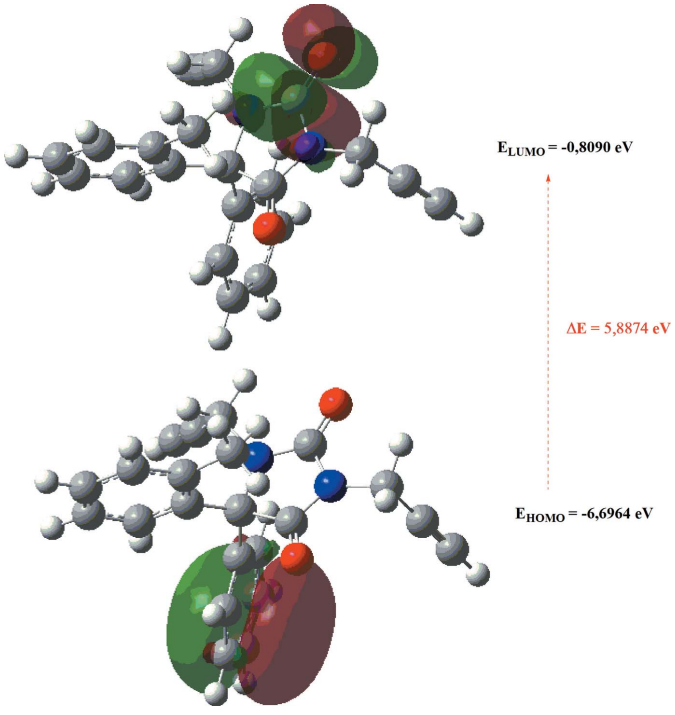

Figure 8
The energy band gap of the title compound.

Table 5
Experimental details.

Crystal data	
Chemical formula	$C_{21}H_{16}N_2O_2$
M_r	328.36
Crystal system, space group	Monoclinic, $P2_1$
Temperature (K)	296
a, b, c (Å)	10.144 (3), 7.952 (2), 10.928 (3)
β (°)	97.104 (12)
V (Å^3)	874.8 (4)
Z	2
Radiation type	Mo $K\alpha$
μ (mm^{-1})	0.08
Crystal size (mm)	0.34 × 0.17 × 0.12
Data collection	
Diffractometer	Bruker APEXII CCD
Absorption correction	Multi-scan (*SADABS*; Bruker, 2016)
T_{min}, T_{max}	0.694, 0.746
No. of measured, independent and observed [$I > 2\sigma(I)$] reflections	21744, 3988, 3529
R_{int}	0.037
(sin $\theta/\lambda)_{max}$ (Å^{-1})	0.650
Refinement	
$R[F^2 > 2\sigma(F^2)]$, $wR(F^2)$, S	0.035, 0.090, 1.03
No. of reflections	3988
No. of parameters	290
No. of restraints	1
H-atom treatment	All H-atom parameters refined
$\Delta\rho_{max}$, $\Delta\rho_{min}$ (e Å^{-3})	0.14, −0.16
Absolute structure	Flack x determined using 1436 quotients $[(I^+)-(I^-)]/[(I^+)+(I^-)]$ (Parsons et al., 2013)
Absolute structure parameter	−0.3 (4)

Computer programs: *APEX3* and *SAINT* (Bruker, 2016), *SHELXT* (Sheldrick, 2015*a*), *SHELXL* (Sheldrick, 2015*b*) and *OLEX2* (Dolomanov *et al.*, 2009).

7. Database survey

A non-alkylated analogue, namely 5,5-diphenylimidazolidine-2,4-dione, has been reported (Camerman & Camerman, 1971), as well as three similar structures, 3-*n*-pentyl-5,5-diphenylimidazolidine-2,4-dione (Guerrab *et al.*, 2017), 3-benzyl-5,5 diphenylimidazolidine-2,4-dione (Guerrab *et al.*, 2018) and 3-[2-(4-fluorophenyl)-2-oxoethyl]-5,5 diphenylimidazolidine-2,4-dione (Mague *et al.*, 2014).

8. Synthesis and crystallization

The appropriate bromide propargil (2.4 ml, 20.0 mmol) was added to a solution of 5,5 diphenylhydantoin (3.52 g, 10.0 mmol) in DMF (50 ml), potassium carbonate (2.76 g, 20.0 mmol) and tetra-*n*-butylammonium bromide (0.32 g,

1.0 mmol) at room temperature. The reaction was monitored using TLC. After removal of the inorganic salt by filtration, the solution was evaporated under reduced pressure. The residue was separated by chromatography on a column of silica gel with ethyl acetate–hexane (*v*:*v* 3:7) as eluent. The isolated solid was crystallized from ethanol solution to afford colourless crystals (yield: 82%).

9. Refinement

Crystal data, data collection and structure refinement details are summarized in Table 5. Hydrogen atoms were located in a difference-Fourier map, and refined freely. The Flack absolute structure parameter (Parsons *et al.*, 2013) was refined; expected values are 0 for the correct and +1 for the inverted absolute structure. The refined value is −0.3 (4) (Sheldrick, 2015*b*). Since the large e.s.d. means that the assignment is not unambiguous, the absolute structure was not determined reliably.

Funding information

TH is grateful to the Hacettepe University Scientific Research Project Unit (grant No. 013 D04 602 004).

References

Amir, M. & Kumar, S. (2005). *Indian J. Chem.* **44B**, 2532–2537.
Badawey, E. A. M. & El-Ashmawey, I. M. (1998). *Eur. J. Med. Chem.* **33**, 349–361.
Becke, A. D. (1993). *J. Chem. Phys.* **98**, 5648–5652.
Bruker (2016). *APEX3*, *SAINT* and *SADABS*. Bruker AXS, Inc., Madison, Wisconsin, USA.
Camerman, A. & Camerman, N. (1971). *Acta Cryst.* B**27**, 2205–2211.
Das, N., Verma, A., Shrivastava, P. K. & Shrivastava, S. K. (2008). *Indian J. Chem.* B**47**, 1555–1558.
Dolomanov, O. V., Bourhis, L. J., Gildea, R. J., Howard, J. A. K. & Puschmann, H. (2009). *J. Appl. Cryst.* **42**, 339–341.
Frisch, M. J., *et al.* (2009). *GAUSSIAN09*. Gaussian Inc., Wallingford, CT, USA.
Guerrab, W., Akrad, R., Ansar, M., Taoufik, J., Mague, J. T. & Ramli, Y. (2017). *IUCrData*, **2**, x171693.
Guerrab, W., Akrad, R., Ansar, M., Taoufik, J., Mague, J. T. & Ramli, Y. (2018). *IUCrData*, **3**, x171832.
Hathwar, V. R., Sist, M., Jørgensen, M. R. V., Mamakhel, A. H., Wang, X., Hoffmann, C. M., Sugimoto, K., Overgaard, J. & Iversen, B. B. (2015). *IUCrJ*, **2**, 563–574.
Higashi, Y., Jitsuiki, D., Chayama, K. & Yoshizumi, M. (2006). *Recent. Patents Cardiovasc. Drug. Discov.* **1**, 85–93.
Hirshfeld, H. L. (1977). *Theor. Chim. Acta*, **44**, 129–138.
Jayatilaka, D., Grimwood, D. J., Lee, A., Lemay, A., Russel, A. J., Taylor, C., Wolff, S. K., Cassam-Chenai, P. & Whitton, A. (2005). *TONTO - A System for Computational Chemistry. Available at: http://hirshfeldsurface.net/*
Mackenzie, C. F., Spackman, P. R., Jayatilaka, D. & Spackman, M. A. (2017). *IUCrJ*, **4**, 575–587.
Mague, J. T., Abdel-Aziz, A. A.-M. & El-Azab, A. S. (2014). *Acta Cryst.* E**70**, o226–o227.
McKinnon, J. J., Jayatilaka, D. & Spackman, M. A. (2007). *Chem. Commun.* pp. 3814–3816.
Naik, C. G. & Malik, C. M. (2010). *Orient. J. Chem.* **26**, 113–116.
Parsons, S., Flack, H. D. & Wagner, T. (2013). *Acta Cryst.* B**69**, 249–259.
Pathak, R. B. & Bahel, S. C. (1980). *J. Indian Chem. Soc.* **57**, 1108–1111.
Pawar, R. A. & Patil, A. A. (1994). *Indian J. Chem.* **33B**, 156–158.
Sahu, S. K., Azam, A. M., Banerjee, M., Choudhary, P., Sutradhar, S., Panda, P. K. & Misra, P. K. (2007). *J. Indian Chem. Soc.* **84**, 1011–1015.
Sheldrick, G. M. (2015*a*). *Acta Cryst.* A**71**, 3–8.
Sheldrick, G. M. (2015*b*). *Acta Cryst.* C**71**, 3–8.
Singh, D. & Singh, D. (1991). *J. Indian Chem. Soc.* **68**, 165–167.
Spackman, M. A. & Jayatilaka, D. (2009). *CrystEngComm*, **11**, 19–32.
Spackman, M. A., McKinnon, J. J. & Jayatilaka, D. (2008). *CrystEngComm*, **10**, 377–388.
Srivalli, T., Satish, K. & Suthakaran, R. (2011). *Int. J. Innov. Pharm. Res.* **2**, 172–174.
Turner, M. J., Grabowsky, S., Jayatilaka, D. & Spackman, M. A. (2014). *J. Phys. Chem. Lett.* **5**, 4249–4255.
Turner, M. J., McKinnon, J. J., Wolff, S. K., Grimwood, D. J., Spackman, P. R., Jayatilaka, D. & Spackman, M. A. (2017). *CrystalExplorer17*. The University of Western Australia.
Turner, M. J., Thomas, S. P., Shi, M. W., Jayatilaka, D. & Spackman, M. A. (2015). *Chem. Commun.* **51**, 3735–3738.
Venkatesan, P., Thamotharan, S., Ilangovan, A., Liang, H. & Sundius, T. (2016). *Spectrochim. Acta Part A*, **153**, 625–636.

supporting information

Acta Cryst. (2019). E**75**, 951-956 [https://doi.org/10.1107/S2056989019007801]

Crystal structure, Hirshfeld surface analysis and interaction energy and DFT studies of 5,5-diphenyl-1,3-bis(prop-2-yn-1-yl)imidazolidine-2,4-dione

Ismail Ghandour, Abdelouahed Bouayad, Tuncer Hökelek, Amal Haoudi, Frédéric Capet, Catherine Renard and Youssef Kandri Rodi

Computing details

Data collection: *APEX3* (Bruker, 2016); cell refinement: *SAINT* (Bruker, 2016); data reduction: *SAINT* (Bruker, 2016); program(s) used to solve structure: SHELXT (Sheldrick, 2015a); program(s) used to refine structure: *SHELXL* (Sheldrick, 2015b); molecular graphics: *OLEX2* (Dolomanov *et al.*, 2009); software used to prepare material for publication: *OLEX2* (Dolomanov *et al.*, 2009).

5,5-Diphenyl-1,3-bis(prop-2-yn-1-yl)imidazolidine-2,4-dione

Crystal data

$C_{21}H_{16}N_2O_2$
$M_r = 328.36$
Monoclinic, $P2_1$
$a = 10.144$ (3) Å
$b = 7.952$ (2) Å
$c = 10.928$ (3) Å
$\beta = 97.104$ (12)°
$V = 874.8$ (4) Å^3
$Z = 2$
$F(000) = 344$
$D_x = 1.247$ Mg m^{-3}
Mo $K\alpha$ radiation, $\lambda = 0.71073$ Å
Cell parameters from 9652 reflections
$\theta = 3.2$–27.2°
$\mu = 0.08$ mm^{-1}
$T = 296$ K
Prism, colourless
0.34 × 0.17 × 0.12 mm

Data collection

Bruker APEXII CCD diffractometer
φ and ω scans
Absorption correction: multi-scan (SADABS; Bruker, 2016)
$T_{min} = 0.694$, $T_{max} = 0.746$
21744 measured reflections
3988 independent reflections
3529 reflections with $I > 2\sigma(I)$
$R_{int} = 0.037$
$\theta_{max} = 27.5°$, $\theta_{min} = 1.9°$
$h = -13\rightarrow13$
$k = -10\rightarrow10$
$l = -13\rightarrow14$

Refinement

Refinement on F^2
Least-squares matrix: full
$R[F^2 > 2\sigma(F^2)] = 0.035$
$wR(F^2) = 0.090$
$S = 1.03$
3988 reflections
290 parameters
1 restraint
Primary atom site location: dual
Hydrogen site location: difference Fourier map
All H-atom parameters refined
$w = 1/[\sigma^2(F_o^2) + (0.0457P)^2 + 0.0829P]$ where $P = (F_o^2 + 2F_c^2)/3$
$(\Delta/\sigma)_{max} < 0.001$
$\Delta\rho_{max} = 0.14$ e Å^{-3}
$\Delta\rho_{min} = -0.16$ e Å^{-3}

Absolute structure: Flack *x* determined using 1436 quotients $[(I^+)-(I^-)]/[(I^+)+(I^-)]$ (Parsons et al., 2013)
Absolute structure parameter: −0.3 (4)

Special details

Geometry. All esds (except the esd in the dihedral angle between two l.s. planes) are estimated using the full covariance matrix. The cell esds are taken into account individually in the estimation of esds in distances, angles and torsion angles; correlations between esds in cell parameters are only used when they are defined by crystal symmetry. An approximate (isotropic) treatment of cell esds is used for estimating esds involving l.s. planes.

Fractional atomic coordinates and isotropic or equivalent isotropic displacement parameters (Å²)

	x	*y*	*z*	U_{iso}*/U_{eq}
O1	0.27390 (15)	0.2664 (2)	0.19321 (15)	0.0502 (4)
O2	−0.01151 (15)	0.7093 (2)	0.18041 (16)	0.0521 (4)
N1	0.10965 (17)	0.4650 (2)	0.16652 (16)	0.0421 (4)
N2	0.20794 (16)	0.6856 (2)	0.26052 (16)	0.0408 (4)
C1	0.30827 (18)	0.5513 (3)	0.27974 (18)	0.0380 (4)
C2	0.2324 (2)	0.4054 (3)	0.20923 (18)	0.0387 (4)
C3	0.09114 (19)	0.6317 (3)	0.20165 (18)	0.0390 (4)
C4	0.33794 (18)	0.5114 (2)	0.41722 (19)	0.0385 (4)
C5	0.2604 (2)	0.3960 (3)	0.4718 (2)	0.0458 (5)
C6	0.2784 (3)	0.3712 (4)	0.5987 (2)	0.0565 (6)
C7	0.3738 (3)	0.4604 (4)	0.6713 (2)	0.0572 (6)
C8	0.4520 (2)	0.5750 (3)	0.6180 (2)	0.0526 (6)
C9	0.4342 (2)	0.6008 (3)	0.4921 (2)	0.0454 (5)
C10	0.42895 (19)	0.5861 (3)	0.21163 (19)	0.0395 (4)
C11	0.5495 (2)	0.5070 (3)	0.2474 (2)	0.0441 (5)
C12	0.6546 (2)	0.5272 (3)	0.1782 (2)	0.0543 (6)
C13	0.6410 (3)	0.6249 (4)	0.0733 (2)	0.0606 (6)
C14	0.5225 (3)	0.7025 (4)	0.0372 (2)	0.0622 (7)
C15	0.4163 (2)	0.6834 (3)	0.1052 (2)	0.0538 (6)
C16	0.0113 (3)	0.3724 (4)	0.0851 (2)	0.0541 (6)
C17	−0.0433 (2)	0.2305 (3)	0.1448 (3)	0.0613 (7)
C18	−0.0849 (4)	0.1125 (5)	0.1895 (5)	0.1046 (14)
C19	0.2236 (3)	0.8536 (3)	0.3129 (2)	0.0504 (5)
C20	0.1674 (3)	0.8738 (4)	0.4290 (3)	0.0701 (8)
C21	0.1218 (5)	0.8918 (10)	0.5191 (5)	0.136 (2)
H5	0.189 (2)	0.328 (3)	0.420 (2)	0.051 (7)*
H6	0.228 (3)	0.296 (4)	0.632 (3)	0.068 (8)*
H7	0.389 (3)	0.445 (4)	0.763 (3)	0.080 (10)*
H8	0.522 (3)	0.636 (4)	0.669 (2)	0.059 (7)*
H9	0.486 (3)	0.677 (4)	0.455 (3)	0.075 (9)*
H11	0.562 (2)	0.435 (4)	0.323 (2)	0.054 (7)*
H12	0.736 (3)	0.474 (4)	0.203 (3)	0.069 (8)*
H13	0.720 (3)	0.641 (4)	0.027 (3)	0.068 (8)*
H14	0.511 (3)	0.777 (4)	−0.037 (3)	0.072 (8)*
H15	0.330 (3)	0.737 (4)	0.076 (3)	0.060 (7)*

H16A	−0.051 (3)	0.446 (4)	0.056 (3)	0.060 (8)*
H16B	0.053 (3)	0.332 (4)	0.014 (3)	0.070 (9)*
H18	−0.113 (6)	0.010 (8)	0.228 (6)	0.18 (2)*
H19A	0.315 (3)	0.879 (4)	0.328 (2)	0.061 (7)*
H19B	0.182 (3)	0.926 (4)	0.250 (3)	0.067 (8)*
H21	0.087 (5)	0.905 (8)	0.590 (5)	0.16 (2)*

Atomic displacement parameters (Å²)

	U^{11}	U^{22}	U^{33}	U^{12}	U^{13}	U^{23}
O1	0.0528 (9)	0.0399 (8)	0.0585 (10)	0.0036 (7)	0.0088 (7)	−0.0076 (7)
O2	0.0430 (8)	0.0499 (9)	0.0606 (10)	0.0084 (7)	−0.0045 (7)	0.0041 (7)
N1	0.0425 (9)	0.0389 (9)	0.0426 (9)	−0.0019 (7)	−0.0033 (7)	−0.0008 (8)
N2	0.0373 (8)	0.0349 (9)	0.0492 (10)	0.0009 (7)	0.0014 (7)	−0.0011 (7)
C1	0.0361 (9)	0.0342 (9)	0.0432 (11)	0.0012 (8)	0.0035 (8)	0.0012 (8)
C2	0.0414 (10)	0.0385 (10)	0.0368 (10)	−0.0003 (8)	0.0070 (8)	0.0009 (8)
C3	0.0396 (10)	0.0403 (11)	0.0365 (10)	0.0013 (8)	0.0024 (8)	0.0058 (8)
C4	0.0349 (9)	0.0385 (11)	0.0423 (11)	0.0052 (8)	0.0055 (8)	0.0012 (8)
C5	0.0414 (11)	0.0468 (12)	0.0501 (12)	0.0006 (9)	0.0094 (9)	0.0032 (10)
C6	0.0574 (13)	0.0592 (15)	0.0556 (14)	0.0074 (12)	0.0183 (11)	0.0142 (12)
C7	0.0644 (15)	0.0677 (16)	0.0400 (12)	0.0230 (13)	0.0082 (10)	0.0047 (11)
C8	0.0531 (12)	0.0545 (14)	0.0476 (13)	0.0104 (11)	−0.0037 (10)	−0.0093 (11)
C9	0.0438 (11)	0.0440 (11)	0.0478 (12)	0.0016 (9)	0.0035 (9)	−0.0013 (9)
C10	0.0386 (9)	0.0391 (11)	0.0412 (10)	−0.0022 (8)	0.0060 (7)	0.0009 (8)
C11	0.0405 (10)	0.0450 (12)	0.0468 (12)	0.0014 (9)	0.0054 (9)	0.0040 (10)
C12	0.0419 (11)	0.0616 (15)	0.0605 (15)	0.0032 (11)	0.0105 (10)	0.0011 (12)
C13	0.0519 (13)	0.0735 (17)	0.0601 (14)	−0.0040 (12)	0.0219 (11)	0.0055 (13)
C14	0.0692 (16)	0.0698 (17)	0.0498 (14)	−0.0003 (13)	0.0166 (12)	0.0179 (13)
C15	0.0482 (12)	0.0622 (15)	0.0507 (13)	0.0044 (11)	0.0053 (10)	0.0129 (12)
C16	0.0540 (13)	0.0525 (14)	0.0520 (14)	−0.0059 (11)	−0.0086 (11)	−0.0047 (12)
C17	0.0463 (12)	0.0490 (14)	0.088 (2)	−0.0035 (10)	0.0067 (12)	−0.0068 (13)
C18	0.081 (2)	0.066 (2)	0.174 (4)	−0.0128 (18)	0.043 (2)	0.017 (2)
C19	0.0479 (13)	0.0358 (11)	0.0664 (15)	0.0013 (9)	0.0025 (11)	−0.0020 (11)
C20	0.0587 (15)	0.0758 (19)	0.0742 (19)	0.0032 (14)	0.0024 (13)	−0.0289 (16)
C21	0.103 (3)	0.214 (6)	0.094 (3)	0.001 (4)	0.026 (2)	−0.069 (4)

Geometric parameters (Å, º)

O1—C2	1.203 (3)	C10—C11	1.388 (3)
O2—C3	1.208 (2)	C10—C15	1.390 (3)
N1—C2	1.360 (3)	C11—C12	1.391 (3)
N1—C3	1.399 (3)	C11—H11	1.00 (3)
N1—C16	1.453 (3)	C12—C13	1.377 (4)
N2—C1	1.472 (3)	C12—H12	0.94 (3)
N2—C3	1.346 (3)	C13—C14	1.366 (4)
N2—C19	1.454 (3)	C13—H13	1.01 (3)
C1—C10	1.534 (3)	C14—H14	1.00 (3)
C2—C1	1.545 (3)	C15—C14	1.390 (4)

C4—C1	1.529 (3)	C15—H15	0.99 (3)
C4—C5	1.390 (3)	C16—H16A	0.89 (3)
C4—C9	1.390 (3)	C16—H16B	0.98 (3)
C5—C6	1.389 (3)	C17—C16	1.447 (4)
C5—H5	1.02 (3)	C17—C18	1.162 (5)
C6—C7	1.370 (4)	C18—H18	0.97 (6)
C6—H6	0.90 (3)	C19—C20	1.462 (4)
C7—H7	1.01 (3)	C19—H19A	0.94 (3)
C8—C7	1.384 (4)	C19—H19B	0.95 (3)
C8—H8	0.98 (3)	C20—C21	1.148 (5)
C9—C8	1.380 (3)	C21—H21	0.90 (5)
C9—H9	0.93 (3)		

O1···H16B	2.84 (2)	C20···C4	3.372 (3)
O1···H13^{i}	2.61 (2)	C20···C9	3.472 (3)
O1···H5	2.767 (18)	C2···H5	2.476 (18)
O1···H8^{ii}	2.62 (2)	C4···H11	2.679 (18)
O2···H18^{iii}	2.68 (5)	C6···H9^{ii}	2.97 (2)
O2···H19B	2.65 (2)	C6···H18^{v}	2.90 (4)
O2···H16A	2.50 (2)	C8···H11^{vi}	2.94 (2)
O2···H16B^{iv}	2.33 (2)	C8···H19A^{ii}	2.83 (2)
N2···H15	2.53 (2)	C9···H11	2.73 (2)
C4···C20	3.372 (3)	C10···H9	2.75 (2)
C9···C19	3.378 (3)	C10···H19A	2.96 (2)
C9···C11	3.138 (3)	C11···H14^{i}	2.94 (2)
C9···C20	3.472 (3)	C11···H9	2.79 (2)
C11···C9	3.138 (3)	C12···H14^{i}	2.91 (2)
C15···C19	3.450 (3)	C14···H7^{vi}	2.97 (2)
C19···C15	3.450 (3)	H8···H11^{vi}	2.53 (3)
C19···C9	3.378 (3)	H9···H11	2.58 (3)

C2—N1—C3	112.60 (17)	C8—C9—H9	121.2 (19)
C2—N1—C16	124.3 (2)	C11—C10—C1	120.65 (18)
C3—N1—C16	122.9 (2)	C11—C10—C15	118.4 (2)
C3—N2—C1	112.90 (16)	C15—C10—C1	120.64 (18)
C3—N2—C19	121.81 (18)	C10—C11—C12	120.2 (2)
C19—N2—C1	124.78 (17)	C10—C11—H11	120.6 (14)
N2—C1—C2	100.41 (15)	C12—C11—H11	119.3 (14)
N2—C1—C4	109.84 (16)	C11—C12—H12	119.8 (18)
N2—C1—C10	112.27 (16)	C13—C12—C11	120.9 (2)
C4—C1—C2	111.07 (16)	C13—C12—H12	119.3 (18)
C4—C1—C10	116.25 (15)	C12—C13—H13	119.5 (17)
C10—C1—C2	105.76 (16)	C14—C13—C12	119.3 (2)
O1—C2—N1	126.3 (2)	C14—C13—H13	121.2 (17)
O1—C2—C1	126.93 (19)	C13—C14—C15	120.6 (2)
N1—C2—C1	106.74 (16)	C13—C14—H14	121.1 (17)
O2—C3—N1	125.0 (2)	C15—C14—H14	118.2 (17)
O2—C3—N2	128.0 (2)	C10—C15—C14	120.7 (2)

N2—C3—N1	107.02 (17)	C10—C15—H15	119.9 (16)
C5—C4—C1	120.41 (18)	C14—C15—H15	119.3 (16)
C9—C4—C1	120.74 (18)	N1—C16—H16A	107.0 (19)
C9—C4—C5	118.6 (2)	N1—C16—H16B	108.8 (17)
C4—C5—H5	121.0 (14)	C17—C16—N1	113.0 (2)
C6—C5—C4	120.7 (2)	C17—C16—H16A	112.0 (18)
C6—C5—H5	118.4 (14)	C17—C16—H16B	108.8 (18)
C5—C6—H6	119 (2)	H16A—C16—H16B	107 (2)
C7—C6—C5	120.0 (2)	C18—C17—C16	177.3 (4)
C7—C6—H6	120.8 (19)	C17—C18—H18	176 (3)
C6—C7—C8	119.8 (2)	N2—C19—C20	114.0 (2)
C6—C7—H7	121.8 (18)	N2—C19—H19A	108.9 (18)
C8—C7—H7	118.3 (18)	N2—C19—H19B	104.8 (18)
C7—C8—H8	120.2 (16)	C20—C19—H19A	107.8 (16)
C9—C8—C7	120.4 (2)	C20—C19—H19B	112.0 (17)
C9—C8—H8	119.3 (16)	H19A—C19—H19B	109 (2)
C4—C9—H9	118.4 (19)	C21—C20—C19	178.8 (5)
C8—C9—C4	120.4 (2)	C20—C21—H21	179 (4)

C3—N2—C1—C4	−112.10 (13)	C2—N1—C3—N2	4.70 (16)
C19—N2—C1—C4	59.82 (18)	C16—N1—C3—N2	−170.68 (14)
C3—N2—C1—C10	116.91 (13)	C9—C4—C5—C6	0.3 (2)
C19—N2—C1—C10	−71.17 (19)	C1—C4—C5—C6	−173.66 (14)
C3—N2—C1—C2	4.97 (15)	C4—C5—C6—C7	−0.3 (3)
C19—N2—C1—C2	176.88 (13)	C5—C6—C7—C8	0.0 (3)
C9—C4—C1—N2	−87.33 (15)	C9—C8—C7—C6	0.3 (3)
C5—C4—C1—N2	86.52 (16)	C4—C9—C8—C7	−0.3 (3)
C9—C4—C1—C10	41.52 (19)	C5—C4—C9—C8	0.0 (2)
C5—C4—C1—C10	−144.63 (14)	C1—C4—C9—C8	173.96 (14)
C9—C4—C1—C2	162.49 (13)	N2—C1—C10—C11	159.40 (13)
C5—C4—C1—C2	−23.66 (18)	C4—C1—C10—C11	31.74 (19)
O1—C2—C1—N2	177.04 (14)	C2—C1—C10—C11	−92.03 (15)
N1—C2—C1—N2	−1.91 (14)	N2—C1—C10—C15	−27.33 (19)
O1—C2—C1—C4	−66.81 (19)	C4—C1—C10—C15	−154.99 (14)
N1—C2—C1—C4	114.23 (13)	C2—C1—C10—C15	81.25 (17)
O1—C2—C1—C10	60.15 (19)	C15—C10—C11—C12	0.6 (2)
N1—C2—C1—C10	−118.80 (12)	C1—C10—C11—C12	174.00 (15)
C3—N1—C2—O1	179.51 (14)	C10—C11—C12—C13	−0.2 (3)
C16—N1—C2—O1	−5.2 (2)	C11—C12—C13—C14	−0.1 (3)
C3—N1—C2—C1	−1.52 (16)	C12—C13—C14—C15	0.0 (3)
C16—N1—C2—C1	173.78 (14)	C10—C15—C14—C13	0.4 (3)
C19—N2—C3—O2	2.4 (2)	C11—C10—C15—C14	−0.7 (3)
C1—N2—C3—O2	174.63 (14)	C1—C10—C15—C14	−174.13 (17)
C19—N2—C3—N1	−178.28 (14)	C2—N1—C16—C17	69.8 (2)
C1—N2—C3—N1	−6.09 (16)	C3—N1—C16—C17	−115.34 (18)

C2—N1—C3—O2	−175.99 (14)	C3—N2—C19—C20	76.6 (2)
C16—N1—C3—O2	8.6 (2)	C1—N2—C19—C20	−94.61 (19)

Symmetry codes: (i) −*x*+1, *y*−1/2, −*z*; (ii) −*x*+1, *y*−1/2, −*z*+1; (iii) *x*, *y*+1, *z*; (iv) −*x*, *y*+1/2, −*z*; (v) −*x*, *y*+1/2, −*z*+1; (vi) −*x*+1, *y*+1/2, −*z*+1.

Hydrogen-bond geometry (Å, º)

*Cg*1 and *Cg*2 are the centroids of the C4–C9 and C10–C15 rings, respectively.

D—H···*A*	*D*—H	H···*A*	*D*···*A*	*D*—H···*A*
C16—H16*B*···O2^{vii}	0.98 (3)	2.33 (3)	3.178 (3)	144 (2)
C9—H9···*Cg*1^{vi}	0.93 (3)	2.93 (2)	3.778 (2)	152.7 (17)
C14—H14···*Cg*2^{viii}	1.00 (3)	2.87 (2)	3.762 (3)	149.6 (17)

Symmetry codes: (vi) −*x*+1, *y*+1/2, −*z*+1; (vii) −*x*, *y*−1/2, −*z*; (viii) −*x*+1, *y*+1/2, −*z*.